Ionic basis of the caesium-induced depolarisation in rat supraoptic nucleus neurones

Masoud Ghamari-Langroudi and Charles W. Bourque

Centre for Research in Neuroscience, Montreal General Hospital and McGill University, 1650 Cedar Avenue, Montreal, QC, Canada H3G 1A4

(Received 7 March 2001; accepted after revision 15 June 2001)

1. The effects of external Cs^+ on magnocellular neurosecretory cells were studied during intracellular recordings from 93 supraoptic nucleus neurones in superfused explants of rat hypothalamus.

2. Bath application of 3–5 mM Cs^+ provoked reversible membrane depolarisation and increased firing rate in all of the neurones tested. Voltage–current analysis revealed an increase in membrane resistance between −120 and −55 mV. The increase in resistance was greater below −85 mV than at more positive potentials.

3. Voltage-clamp analysis showed that external Cs^+ blocked the hyperpolarisation-activated inward current, I_H. Under current clamp, application of ZD 7288, a selective blocker of I_H, caused an increase in membrane resistance at voltages $\leqslant -65$ mV. Voltage–current analysis further revealed that blockade of I_H caused hyperpolarisation when the initial voltage was < -60 mV but had no effect at more positive values.

4. Current- and voltage-clamp analysis of the effects of Cs^+ in the presence of ZD 7288, or ZD 7288 and tetraethyl ammonium (TEA), revealed an increase in membrane resistance throughout the range of voltages tested (−120 to −45 mV). The current blocked by Cs^+ in the absence of I_H was essentially voltage independent and reversed at −100 mV. The reversal potential shifted by +22.7 mV when external $[K^+]$ was increased from 3 to 9 mM. We conclude that, in addition to blocking I_H, external Cs^+ blocks a leakage K^+ current that contributes significantly to the resting potential of rat magnocellular neurosecretory cells.

Hypothalamic magnocellular neurosecretory cells (MNCs) are responsible for the release of either vasopressin or oxytocin into the blood (Poulain & Wakerley, 1982). Following their synthesis in MNC somata, these peptides are packaged in vesicles and transported to axon terminals in the neurohypophysis (Brownstein *et al.* 1980) where secretion is triggered by the arrival of action potentials (Dreifuss *et al.* 1971). Previous work has established that different rates and patterns of firing evoked by stimuli affecting MNCs have a profound impact on excitation–secretion coupling (e.g. Dutton & Dyball, 1979; Bicknell & Leng, 1981; Bicknell, 1988). Changes in firing rate and pattern, therefore, are both important features of the response of these neurones to physiological and pathological conditions. In both types of MNC, action potentials are initiated at the soma as a result of interactions between afferent synaptic signals and intrinsic membrane properties (Renaud & Bourque, 1991). Since the integrative properties of the membrane are governed by the complement, density and distribution of ion channels within the somato-dendritic compartment, increasing attention is being placed on the identification and characterisation of the membrane channels expressed in MNCs (for review see Hatton & Li, 1998).

Experiments on hypothalamic slices have previously shown the presence of the hyperpolarisation-activated inward current (I_H) in guinea-pig MNCs (Erickson *et al.* 1993). Although this study revealed an involvement of I_H in the control of burst firing, the presence and significance of I_H in rat MNCs remained somewhat controversial for two primary reasons. First, experiments using rat hypothalamic explants showed that application of external Cs^+, a well-known blocker of I_H (Halliwell & Adams, 1982; Pape, 1996), depolarises MNCs (Stern & Armstrong, 1997; Ghamari-Langroudi & Bourque, 1998). Since blockade of active I_H normally leads to hyperpolarisation (e.g. Maccaferri & McBain, 1996), the occurrence of a depolarising effect of Cs^+ in rat MNCs seemed inconsistent with a presumed presence of I_H. Second, the hallmark features of I_H are (i) that it activates slowly during hyperpolarising steps (hundreds of milliseconds) and (ii) that its amplitude increases during steps to more negative potentials (Halliwell & Adams,

1982). Thus, in current-clamped cells expressing I_H, voltage responses to hyperpolarising current pulses typically feature slow depolarising sags whose amplitudes increase with hyperpolarisation (McCormick & Pape, 1990). However, experiments on rat MNCs held at voltages near threshold have revealed depolarising sags whose amplitudes first increase and then decrease in response to hyperpolarising pulses of increasing amplitude (e.g. Stern & Armstrong, 1996, 1997). Despite these seemingly paradoxical observations, we revealed recently that rat MNCs do express a significant density of I_H and that this current plays an excitatory role in the regulation of electrical activity (Ghamari-Langroudi & Bourque, 2000). Our analysis further suggested that the unusual behaviour of depolarising sags in rat MNCs held near threshold is probably due to the fact that the sags reflect not only the progressive activation of I_H, but also the deactivation of the K^+ current responsible for sustained outward rectification (Stern & Armstrong, 1997).

Although these observations have highlighted the complex interactions that result from the presence of overlapping voltage-sensitive currents at sub- and near-threshold potentials, the basis for the depolarising effects of Cs^+ in rat MNCs remains unknown. Moreover, the robust depolarising effect of external Cs^+ suggests that the presence of a conductance distinct from I_H can also significantly modulate the electrical activity of these neurosecretory neurones. In this study, therefore, we investigated the ionic basis for the depolarising effects of external Cs^+ in rat MNCs. Our results indicate that Cs^+ blocks both I_H and a leakage K^+ current that contributes significantly to the resting potential.

METHODS

Preparation of superfused explants

Hypothalamic explants were prepared as described previously (Ghamari-Langroudi & Bourque, 1998, 2000). Briefly, male Long–Evans rats (150–300 g) were briefly (5–10 s) restrained in a soft, disposable, plastic cone (Harvard Apparatus Canada, Saint-Laurent, QC, Canada) and killed by decapitation using a small rodent guillotine (model 51330; Stoelting Company, Wood Dale, IL, USA). This tissue-harvesting protocol was approved by the Animal Care Committee of McGill University. The brain was then rapidly removed from the cranial vault. A block of tissue (~8 mm × 8 mm × 2 mm) comprising the basal hypothalamus was excised using razor blades and pinned, ventral side up, to the slanted (~30 deg) Sylgard base of a temperature-controlled (32–34 °C) superfusion chamber. Within 2–3 min of decapitation, explants were being superfused (0.5–1 ml min^{-1}) with an oxygenated (95% O_2–5% CO_2) artificial cerebrospinal fluid (ACSF; see below) delivered via a Tygon tube placed over the medial tuberal region. The arachnoid membranes covering the ventral surface of the supraoptic nucleus were removed using fine forceps and a cotton wick was placed at the rostral tip of the explant to facilitate drainage of ACSF.

Solutions and drugs

The ACSF (pH 7.4; 295 ± 1 mosmol kg^{-1}) was composed of (mM): NaCl, 121; $MgCl_2$, 1.3; KCl, 3; $NaHCO_3$, 26; glucose, 10; $CaCl_2$, 2.5 (all from Fisher Scientific Company, Pittsburgh, PA, USA). The ACSF was supplemented, where indicated in the text, with 0.3–0.6 μM tetrodotoxin (TTX; Sigma Chemical Co., St Louis, MO, USA). The effects of Cs^+ were examined by diluting a 1 M stock of CsCl (in H_2O) into ACSF stored in a secondary reservoir (50 ml), and by switching the supply to the delivery tube between the control and secondary reservoir. The I_H blocker ZD 7288 (from Tocris Cookson Inc., Ballwin, MO, USA) was prepared as a 30 mM stock solution (in H_2O) and stored at 4 °C. The effects of ZD 7288 were examined by bath application of ACSF containing a dilution of the stock solution as described above. In experiments examining the effects of Cs^+ in the presence of different concentrations of extracellular K^+, several accessory reservoirs were used to allow the control and Cs^+-containing solutions to carry the same concentration of K^+.

Electrophysiology

Intracellular recordings were obtained using sharp micropipettes prepared from glass capillary tubes (1.2 mm o.d.; A. M. Systems Inc., Everett, WA, USA) pulled on a P87 Flaming-Brown puller (Sutter Instruments Co., Novato, CA, USA). Pipettes were filled with 2 M potassium acetate, yielding a DC resistance of 70–150 MΩ relative to a Ag–AgCl wire electrode immersed in ACSF. Recordings of membrane voltage (DC to 5 kHz) and current (DC to 0.3 kHz) were obtained through an Axoclamp 2A amplifier (Axon Instruments Inc., Foster City, CA, USA). Voltage recordings were performed in continuous current-clamp ('bridge') mode whereas current recordings were performed using the discontinuous single-electrode voltage-clamp (dSEVC) mode. Switching frequencies in dSEVC mode were adjusted (2–3.5 kHz) to ensure that a complete decay of the electrode potential was achieved between periods of current injection. Signals acquired during each experiment were displayed on a chart recorder and digitised (44 kHz; Neurodata Instruments Co., Delaware Water Gap, PA, USA) for back-up storage onto videotape. Current and voltage pulses were delivered through an external pulse generator, or via a Digidata 1200-B interface driven by Clampex 8.0 software (Axon Instruments Inc.) running on a Pentium III computer. All signals were digitised online at 10 kHz and stored on the computer's hard drive. Averaging of current traces and digital subtraction were performed offline using Clampfit 8.0 software.

Statistics

Throughout the paper, group data are reported as means plus or minus the standard error of the mean (±S.E.M.). Differences between mean values recorded under control and test conditions were evaluated using Student's paired t test and differences were considered significant when $P < 0.05$.

Analysis of I_H and G_H (hyperpolarisation-activated conductance)

The properties of I_H evoked by steps to different voltages were derived from an analysis of the Cs^+-sensitive, time-dependent currents revealed by subtracting current traces recorded in the presence of Cs^+ from traces recorded in control conditions. The time-dependent current was fitted using a monoexponential function using Clampfit 8 software. The amplitude of the evoked I_H was defined as the difference between starting and steady-state current values and the time constant of activation was derived directly from the best fit through the data points.

The voltage dependency of G_H can be assessed experimentally by plotting the relative amplitude of current tails evoked at a fixed potential following pulses delivered to different conditioning potentials (e.g. McCormick & Pape, 1990). In MNCs, however, relatively large currents are activated or deactivated upon the termination of voltage steps to negative potentials. In particular, the amplitude of the transient K^+ current measured at −50 mV following a prepulse to −120 mV can exceed 1.5 nA (Bourque, 1988), a value about one hundred times greater than that of the I_H tail expected to result from the same protocol. We therefore estimated G_H as done previously

(Ghamari-Langroudi & Bourque, 2000), from the amplitude of I_H measured at various test voltages (V) divided by the driving force ($V - E_H$), where E_H is the reversal potential of I_H. Moreover, since we could not measure E_H directly, the value was arbitrarily set at −35 mV, a value reflecting the median E_H reported during sharp electrode voltage-clamp studies in a variety of cell types (Pape, 1996). Normalised values of G_H (% G_H) were calculated as: % $G_H = 100 \times G_{H(V)}/G_{H(max)}$, where $G_{H(V)}$ is the value of G_H at voltage V, and where $G_{H(max)}$ is defined as the value of G_H at −120 mV. The data were fitted using a Boltzmann equation:

$$\% G_H = 100/(1 + \exp(V - V_{½}/k)),$$

using Sigmaplot 5 software (Jandel Scientific, San Rafael, CA, USA), where $V_{½}$ is the half-maximal voltage and k is the slope factor characterising the relationship.

RESULTS

The data presented below were obtained during intracellular recordings made from 93 supraoptic nucleus neurones impaled with sharp microelectrodes in superfused explants of rat hypothalamus. These cells had resting membrane potentials more negative than −50 mV, input resistances exceeding 150 MΩ, and fired action potentials whose amplitudes were greater than 60 mV when measured from baseline. Each of these cells also displayed frequency-dependent spike broadening (Andrew & Dudek, 1985; Bourque & Renaud, 1985) and transient outward rectification (Bourque, 1988) when examined from initial membrane potentials below, i.e. negative to, −75 mV. These combined characteristics have been shown to be specific to hypothalamic magnocellular neurosecretory neurones, but not to neighbouring non-neuroendocrine cells, during intracellular recordings *in vitro* (Renaud & Bourque, 1991; Tasker & Dudek, 1991) and *in vivo* (Bourque & Renaud, 1991; Dyball *et al.* 1991).

Effects of external Cs^+ on membrane potential and spike discharge

Previous studies have shown that during current-clamp recordings from MNCs held at membrane potentials below the threshold for action potential discharge, bath application of 2–5 mM Cs^+ causes a steady-state membrane depolarisation (Stern & Armstrong, 1997; Ghamari-Langroudi & Bourque, 1998). We therefore investigated whether external Cs^+ could significantly affect the firing of action potentials. When tested on 15 spontaneously active MNCs, bath application of 3–5 mM external Cs^+ caused a consistent and reversible membrane depolarisation with a mean amplitude of 5.6 ± 0.6 mV (e.g. Fig. 1*A*). This effect was accompanied by a 5.4-fold increase in the mean (±S.E.M.) frequency of firing from 0.34 ± 0.07 Hz in the control to 1.84 ± 0.35 Hz in the presence of Cs^+ ($P < 0.05$). As illustrated in Fig. 1*B*, bath application of Cs^+ (3–5 mM) to silent MNCs (membrane potential (V_m) between −55 and −70 mV) also consistently and reversibly depolarised all of the cells tested (6.1 ± 0.4 mV, $n = 39$). In 27 (69 %) of these cells the Cs^+-induced membrane depolarisation reached the threshold for action potential discharge and the mean peak firing rate achieved in the presence of Cs^+ was 1.3 ± 0.2 Hz. In six MNCs the depolarising effects of Cs^+ were examined both in the control solution and in ACSF containing TTX (0.3–0.6 μM) to block Na^+-dependent action potentials. As illustrated in Fig. 1*B*, the depolarising effects of Cs^+ persisted in the presence of TTX. Moreover, response amplitudes were not significantly

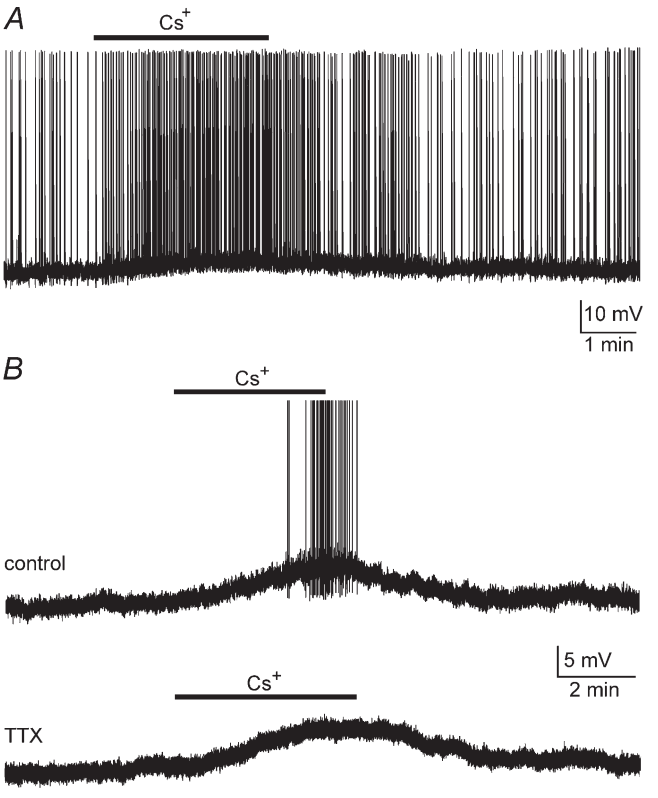

Figure 1. Effects of extracellular Cs^+ on membrane potential and firing rate

A, chart recording of a spontaneously active supraoptic MNC impaled in a superfused explant of rat hypothalamus. Bath application of 3 mM Cs^+ (bar) provoked a reversible membrane depolarisation accompanied by an increase in firing rate. *B*, chart recordings from another supraoptic neurone in which the initial membrane potential was adjusted to −61 mV by continuous injection of hyperpolarising current (−30 pA). Bath application of 3 mM Cs^+ in ACSF (bar; upper trace) provoked a reversible membrane depolarisation and the appearance of action potential discharge. Action potentials are truncated in this panel. The lower trace shows the response of the same cell in ACSF containing 0.6 μM tetrodotoxin (TTX) to block Na^+-dependent action potentials.

different in the two conditions ($P < 0.05$; paired t test), indicating that the Cs^+-evoked depolarisation resulted from an effect on the postsynaptic cell membrane rather than from a presynaptic action.

Effects of Cs^+ on steady-state voltage–current properties

As suggested, the intrinsic membrane properties of MNCs appear to be the target of action of Cs^+. The possible effects of Cs^+ on membrane conductance, therefore, were examined by studying voltage–current (V–I) relationships in control and in the presence of 3–5 mM Cs^+ in five MNCs. For this purpose, the initial membrane potential of each cell was current clamped 5–15 mV below the threshold for spike discharge and steady-state V–I relationships were obtained by injecting square current pulses (1–3 s) of varying amplitude (+50 to −400 pA) at intervals ⩾ 8 s (e.g. Fig. 2*A*). The absolute voltage at the end of each pulse was then measured and plotted as a function of the corresponding absolute current. As illustrated in Fig. 2*B*, steady-state V–I relationships recorded in the presence of Cs^+ exhibited an increase in slope compared to the control, and a reversal potential near −85 mV. The increase in slope (i.e. membrane resistance) suggested that the main effect of Cs^+ was to inhibit one or more of the conductances that were active under steady-state conditions. Since changes in steady-state voltage provoked by Cs^+ (ΔV_{Cs}) at any initial voltage (V_i) partly reflected the magnitude of the Cs^+-sensitive conductance at that particular voltage, a qualitative description of the voltage dependency of the affected currents was derived by examining the relationship between ΔV_{Cs} and V_i. As shown in Fig. 2*C*, the mean (±S.E.M.) values of ΔV_{Cs} were not linearly related to V_i but were more pronounced at voltages below −85 mV. The depolarising effects of Cs^+, therefore, were due either to the inhibition of an inwardly rectifying current reversing near −85 mV, or to the suppression of multiple currents whose different voltage sensitivities and reversal potentials combined to generate the plot shown in Fig. 2*C*. When examined below −100 mV, where the relationship between ΔV_{Cs} and V_i was essentially linear, the slope of the steady-state V–I relationships obtained from MNCs showed a 71 % increase from 177 ± 29 MΩ in control to 304 ± 49 MΩ in the presence of Cs^+ ($P < 0.05$; $n = 5$).

Cs^+ blocks I_H

One of the inwardly rectifying currents that is known to be blocked by external Cs^+ is the hyperpolarisation-activated inward current, I_H (Halliwell & Adams, 1982; Pape, 1996). However, as explained earlier, blockade of the inward current mediated by I_H normally leads to hyperpolarisation (e.g. Maccaferri & McBain, 1996), not depolarisation. Moreover, the graphs in Fig. 2*B* and *C* implied that the depolarising effect of Cs^+ above −85 mV was due to the blockade of an active outward current,

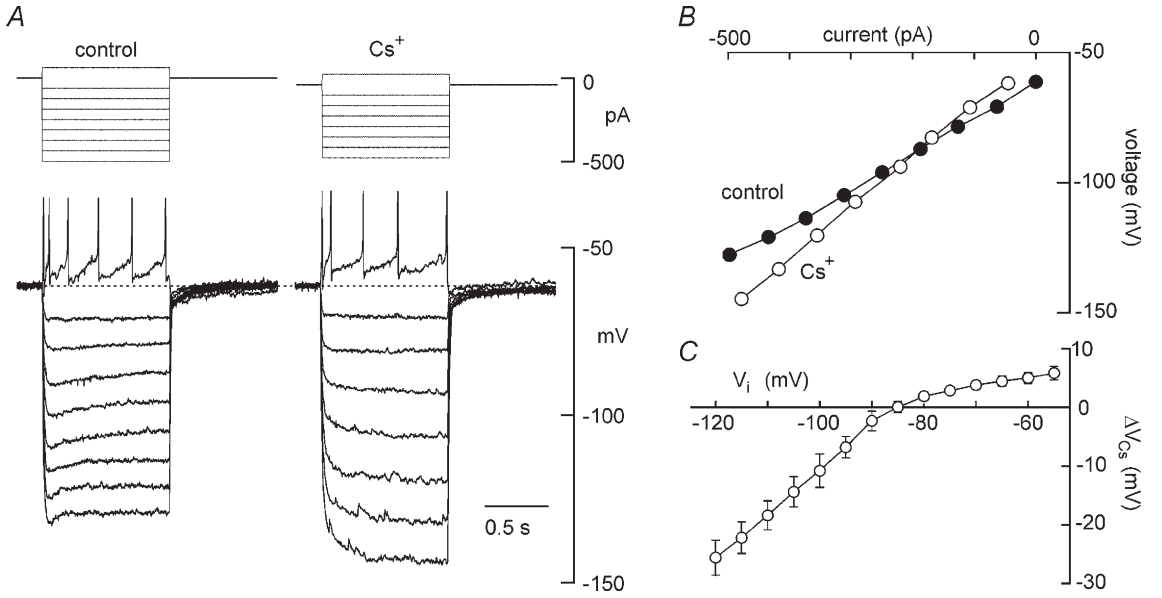

Figure 2. Voltage–current analysis of the Cs^+-mediated depolarisation

A, voltage responses (lower traces) to current pulses (upper) applied in the absence (control) and presence of 3 mM Cs^+. All samples digitised in the last 100 ms of the voltage responses to each current pulse were averaged to determine steady-state voltage. *B*, plot of the steady-state voltage, measured in the absence and presence of Cs^+, as a function of the absolute current being injected into the cell. Using graphs such as these, changes in voltage provoked by Cs^+ (ΔV_{Cs}) at different initial voltages (V_i) were measured as the vertical difference (in mV) between the control and Cs^+ curves, at 5 mV increments. *C*, a plot of mean (±S.E.M.) ΔV_{Cs}– V_i data measured in 5 different MNCs. Note that the plot shows strong inward rectification and a reversal of polarity near −85 mV.

rather than to the recruitment of an additional inward current. We therefore hypothesised that Cs^+ was blocking a current other than I_H to cause depolarisation and that its effects on steady-state V–I relationships reflected actions on both conductances. An alternative hypothesis was that Cs^+ did not block I_H in rat MNCs and that the graph in Fig. 2*C* entirely reflected the properties of the conductance that was blocked by Cs^+ to provoke depolarisation. We thus sought to determine whether Cs^+ effectively blocked I_H in rat MNCs using voltage-clamp analysis. Current–voltage (I–V) relationhips were obtained by delivering a series of prolonged (2–3 s) voltage steps to values between −115 and −40 mV at sufficiently low frequency (⩽ 0.05 Hz) to allow complete inter-pulse deactivation of voltage-sensitive currents. Such trials were performed at constant intervals before, during and after application of Cs^+ (Fig. 3*A*). Digital subtraction of current traces recorded in the presence of Cs^+ from those obtained in control yielded a family of current traces reflecting the time-dependent, Cs^+-sensitive current (i.e. putative I_H) recorded at each voltage (Fig. 3*B*). These traces were fitted with a single exponential function and the time constant of activation (τ_H) and steady-state amplitudes were measured at each of the voltages tested. These data were averaged across the population of cells tested ($n = 5$) and plotted as a function of voltage. The mean current–voltage (I–V) relationship obtained indicated that the time- and voltage-dependent inward current blocked by Cs^+ had an apparent activation threshold near −60 mV (Fig. 3*C*). For each cell the conductance–voltage (G–V) relationship was obtained and the average G–V data were fitted with a Boltzmann equation (see Methods for details). As shown in Fig. 3*D*, the mean G–V relationship revealed a half-activation voltage ($V_{½}$) of −76 mV, and a slope factor (k) of 12. These values are in excellent agreement with results obtained in a previous study of MNCs ($V_{½} = -78$ mV, $k = 12$; Ghamari-Langroudi & Bourque, 2000) using ZD 7288, a selective blocker of I_H (Harris & Constanti, 1995). Moreover, when examined between −120 and −80 mV, τ_H of the time-dependent, Cs^+-sensitive current varied from 125 ± 17 to 470 ± 123 ms, respectively (Fig. 3*E*). These values are also similar to those reported for I_H blocked by ZD 7288 (123 ± 25 to 563 ± 87 ms; Ghamari-Langroudi & Bourque, 2000). External Cs^+, therefore, is an effective blocker of I_H in rat MNCs.

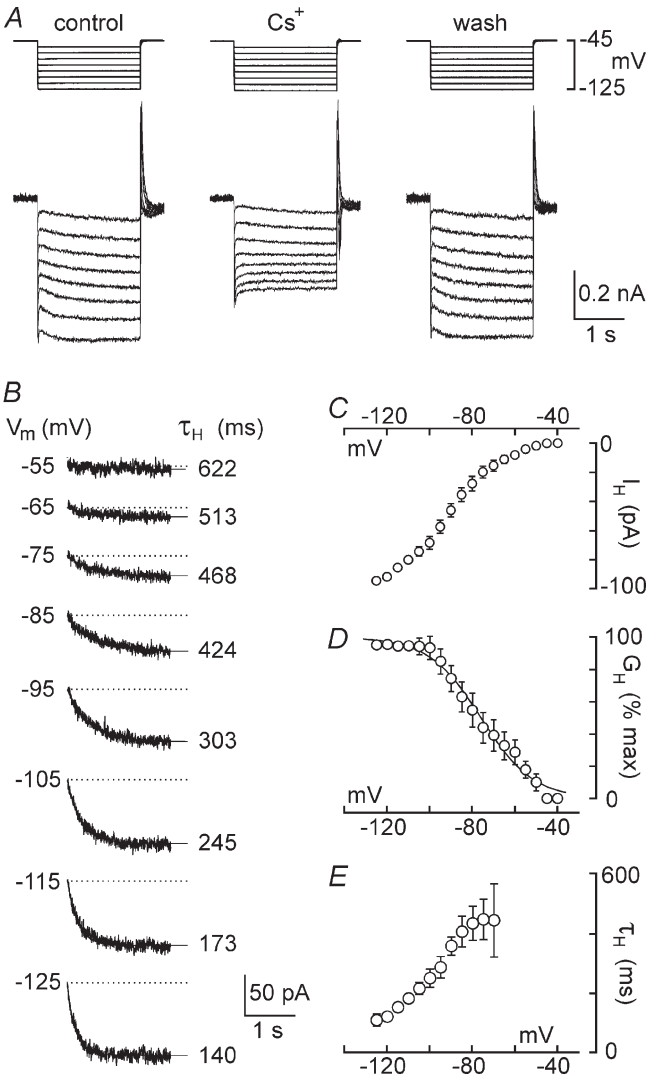

Figure 3. Cs^+ blocks I_H in rat MNCs

Voltage-clamp recordings were made of the membrane currents evoked by voltage steps lasting 2.5 s to a variety of potentials (V_m) between −50 and −125 mV. Multiple trials were evoked in the absence and presence of Cs^+, and current traces recorded in each condition were averaged to reduce noise. *A*, superimposed current traces (lower) resulting from voltage steps (upper) applied before (control), during (Cs^+) and after (wash) application of 5 mM Cs^+. All traces were obtained by averaging 3 individual trials in each condition. *B*, the Cs^+-sensitive, time-dependent currents recorded at each V_m (noted at the left of each trace) obtained by digitally subtracting traces recorded in the presence of Cs^+ from control traces. Superimposed on each trace is a monoexponential fit of the data points (thin line extending beyond the trace). The amplitude (difference between the end of the fit and the dotted line) and time constant of activation of the time-dependent current (τ_H; noted at the right of each trace) were derived from the fits. *C*, mean (±S.E.M.) current–voltage relationship of the Cs^+-sensitive, time-dependent current (I_H) recorded from 4 MNCs. *D*, mean conductance (G_H)–voltage relationship derived from the data shown in *C*. The points are superimposed by a Boltzmann distribution (see Methods for details). *E*, plot of the mean (±S.E.M.) values of τ_H as a function of voltage. Note that activation kinetics accelerate with hyperpolarisation.

Contribution of I_H to the Cs^+-induced inward rectification

Since Cs^+ effectively blocked I_H in rat MNCs, then part or all of the apparent inward rectification observed in Fig. 2*C* could be due to the blockade of I_H. We therefore examined the specific effects of blocking I_H on the *V–I* properties of five MNCs. As illustrated in Fig. 4*A*, bath application of the selective blocker of I_H ZD 7288

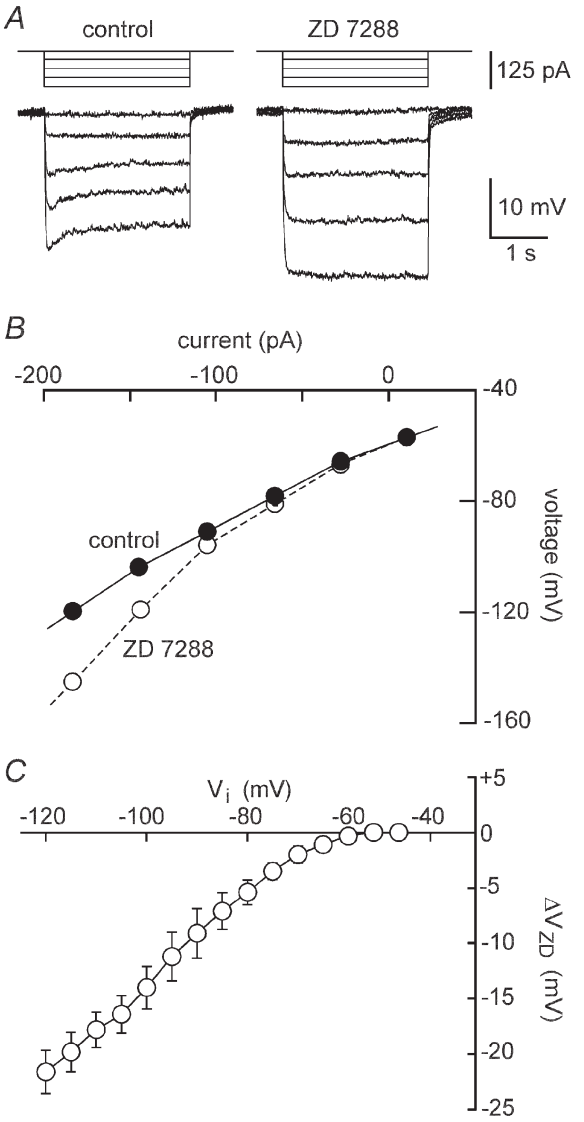

Figure 4. Voltage–current analysis of I_H blockade

A, voltage responses (lower) to 2.5 s current pulses (upper) were recorded from a MNC in the absence (control) and presence of 66 μM ZD 7288. Holding potential was −65 mV. *B*, the plots show the absolute steady-state voltages achieved in response to current pulses delivered in each of the conditions. *C*, the graph shows the mean (±S.E.M.) amplitude of voltage changes evoked by ZD 7288 (ΔV_{ZD}) as a function of control steady-state voltage (V_i) in 5 MNCs. Note the strong inward rectification at negative voltages and that application of ZD 7288 has no effect on V_i at potentials ⩾ −60 mV.

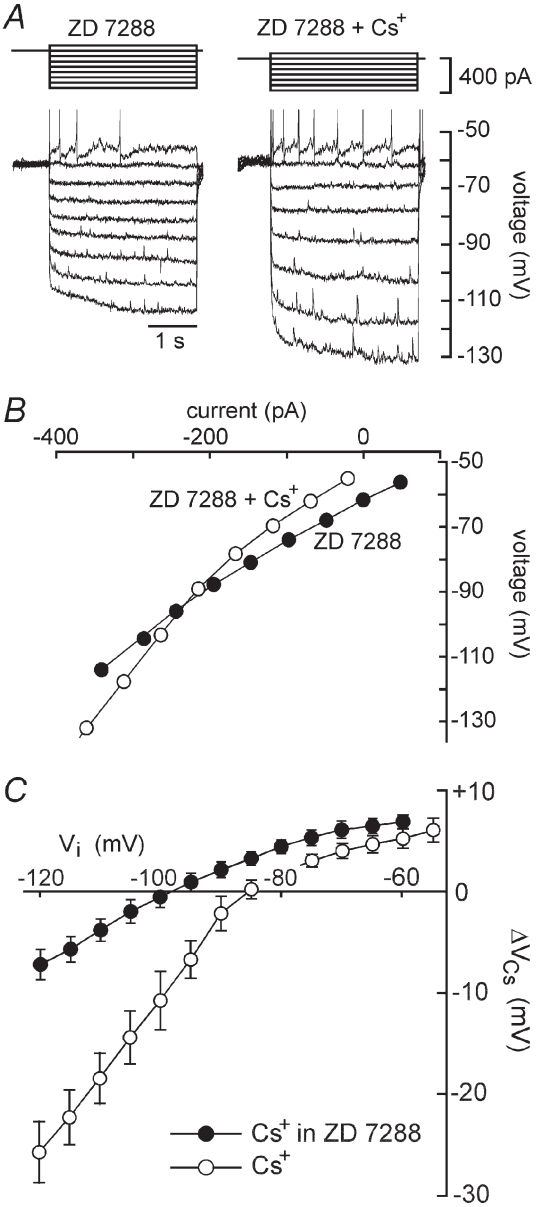

Figure 5. Effects of Cs^+ on membrane potential in the absence of I_H

A, superimposed voltage responses (lower) to 3 s current pulses (upper) applied in the absence (control) and presence of 3 mM Cs^+ (66 μM ZD 7288 was present throughout). *B*, the plots show the absolute steady-state voltages achieved in response to current pulses delivered in each of the conditions shown in *A*. *C*, filled circles plot the mean (±S.E.M.) amplitude of the voltage changes evoked by Cs^+ (ΔV_{Cs}), as a function of control voltage (V_i), in the presence of ZD 7288. The data were measured in 9 different MNCs as described in Fig. 2*B*, from plots such as that shown in *B*. Note that the plot shows much less rectification in the presence than in the absence of ZD 7288 (open circles, data from Fig. 2*C*), and that the reversal potential of the effect lies near −100 mV.

(30–70 μM; Harris & Constanti, 1995) caused a significant increase in the amplitude of voltage responses to prolonged (2–3 s) hyperpolarising current pulses. When examined below −100 mV, the slope of the *V–I* relationship obtained from MNCs showed a 28 % increase from 172 ± 19 MΩ in control to 221 ± 27 MΩ in the presence of ZD 7288 ($P = 0.024$; $n = 5$; e.g. Fig. 4*B*). An examination of the mean voltage changes evoked by ZD 7288 (ΔV_{ZD}) at each V_i led to the plot shown in Fig. 4*C*. The graph suggests that the blockade of I_H provoked a hyperpolarising effect of increasing magnitude at values of V_i below −60 mV, but that it had no effect above −60 mV. These effects were consistent with the voltage dependency of I_H shown in Fig. 3*C*, and they revealed that the inhibition of I_H by Cs^+ could have contributed part or all of the apparent inward rectification observed in Fig. 2*C*.

Effects of Cs^+ on *V–I* properties in the absence of I_H

The voltage dependency of the Cs^+-sensitive current responsible for membrane depolarisation was examined by performing steady-state *V–I* analysis in the absence of I_H. When tested on nine MNCs pre-exposed to 30–70 μM ZD 7288, application of 3–5 mM Cs^+ caused a mean depolarisation of 6.3 ± 0.9 mV. Under these conditions, steady-state *V–I* relationships measured in the absence and presence of Cs^+ revealed an increase in slope resistance that appeared to prevail across the entire range of voltages tested (Fig. 5*A* and *B*). Indeed, in the presence of ZD 7288 mean values of ΔV_{Cs} varied as a more linear function of V_i than in the absence of the drug (Fig. 5*C*). When measured at values negative to −100 mV and in the continuous presence of ZD 7288, the slope resistance of MNCs increased from 204 ± 11 to 281 ± 20 MΩ upon applying Cs^+ ($P < 0.05$; $n = 9$). Finally, the polarity of the voltage changes evoked by Cs^+ in the absence of I_H reversed around −99 mV, a value approximating the equilibrium potential for K^+ ions observed previously under similar recording conditions (Kirkpatrick & Bourque, 1996).

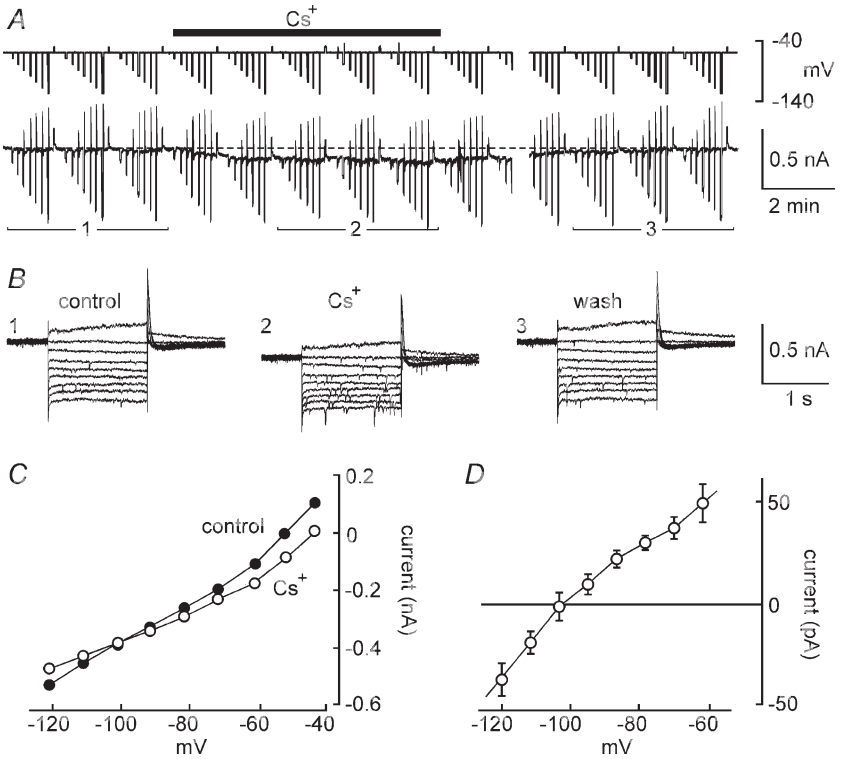

Figure 6. *I–V* analysis of the ZD 7288-resistant, Cs^+-sensitive current

A, chart recording of membrane current (lower) and voltage (upper) in a voltage-clamped MNC. Vertical deflections are changes in voltage and current associated with repeated series of computer-generated steps for *I–V* analysis. The cell was continuously exposed to 66 μM ZD 7288 and the effects of bath application of 3 mM Cs^+ (bar) were examined. Note the steady-state inward current evoked in the presence of Cs^+, and that a gap (5 min) is inserted in the recording. *B*, superimposed current responses to 1.5 s steps to voltages between −120 and −45 mV (holding potential, −50 mV) before (1, control), during (2, Cs^+) and after (3, wash) the application of 3 mM Cs^+. The traces shown represent the digitally averaged ($n = 3$ trials) responses recorded during the corresponding periods numerically identified in *A*. *C*, steady-state *I–V* relationships obtained from the data in *B*. *D*, graph showing the mean (±S.E.M.) difference current plots measured in 4 MNCs. The points represent the voltage dependency of the steady-state current blocked by Cs^+ in the presence of ZD 7288.

Analysis of the Cs^+-sensitive current in the absence of I_H

The results described previously suggested that the depolarising effects of extracellular Cs^+ in MNCs might be due to the inhibition of a steady-state K^+ current lacking significant voltage dependency. We therefore examined the properties of the Cs^+-sensitive, ZD 7288-resistant current under voltage clamp. As illustrated in Fig. 6*A*, bath application of 3–5 mM Cs^+ to MNCs pre-exposed to ZD 7288 and TTX evoked a reversible inward current when cells were clamped at a voltage near −50 mV. Steady-state *I–V* analysis was performed in the absence and presence of 3–5 mM Cs^+ by examining averaged current responses to clamp steps (1–2 s long; every 8–16 s) to a variety of voltages (e.g. Fig. 6*B*). The amplitude of the current responses evoked in each condition was plotted as a function of command potential (Fig. 6*C*) and for each cell a graph of the difference current amplitude was constructed. As illustrated in Fig. 6*D*, the mean ($n = 4$) Cs^+-sensitive (i.e. difference) current underlying the depolarisation of MNCs showed weak inward rectification and a reversal potential near −100 mV. In three cells, measurements of Cs^+-evoked responses were repeated while explants were superfused with ACSF containing alternately 3 and 9 mM $[K^+]_o$ (as well as 35 μM ZD 7288). In the presence of 9 mM $[K^+]_o$ the reversal potential of the Cs^+-evoked depolarisation was shifted by +22.7 ± 2.6 mV compared to values recorded in 3 mM $[K^+]_o$ ($P < 0.05$; data not shown). This value was reasonably close to the shift predicted by the Nernst equation (+28.7 mV) for a K^+-selective membrane at our recording temperature, confirming that the Cs^+-evoked depolarisation is mediated by the suppression of a K^+ conductance.

Externally applied TEA is well known to block the outward currents flowing through a variety of K^+ channels. We therefore examined whether the depolarising effects of Cs^+ could be occluded by TEA. Intracellular recordings were obtained from MNCs in explants superfused with solutions containing 3–5 mM TEA. In each of three MNCs tested under current clamp, bath application of 3 mM Cs^+ still provoked reversible membrane depolarisations (e.g. Fig. 7*A*). When tested under voltage clamp ($n = 5$), application of Cs^+ in the presence of 3–5 mM TEA and 60–70 μM ZD 7288 induced an inward current at voltages near rest, and a decrease in slope conductance (Fig. 7*B* and *C*). In the presence of TEA and in absence of I_H, the mean decrease in slope conductance observed in five MNCs was 0.80 ± 0.16 nS, a value not significantly different from that observed without TEA ($P > 0.05$). The K^+ channels responsible for the depolarising effects of Cs^+, therefore, are not sensitive to 3–5 mM TEA.

DISCUSSION

It has been known for some time that hyperpolarising steps activate a slow inward current in MNCs (Bourque, 1987). Although this behaviour might have been surmised to reflect the presence of I_H, recently published observations appeared to contradict the possible presence of this current in rat MNCs. Indeed, current-clamp experiments in hypothalamic explants (Stern & Armstrong, 1997; Ghamari-Langroudi & Bourque, 1998) revealed that application of external Cs^+, a well-known blocker of I_H (Halliwell & Adams, 1982; Mayer & Westbrook, 1983), causes a membrane depolarisation instead of the hyperpolarisation expected to result

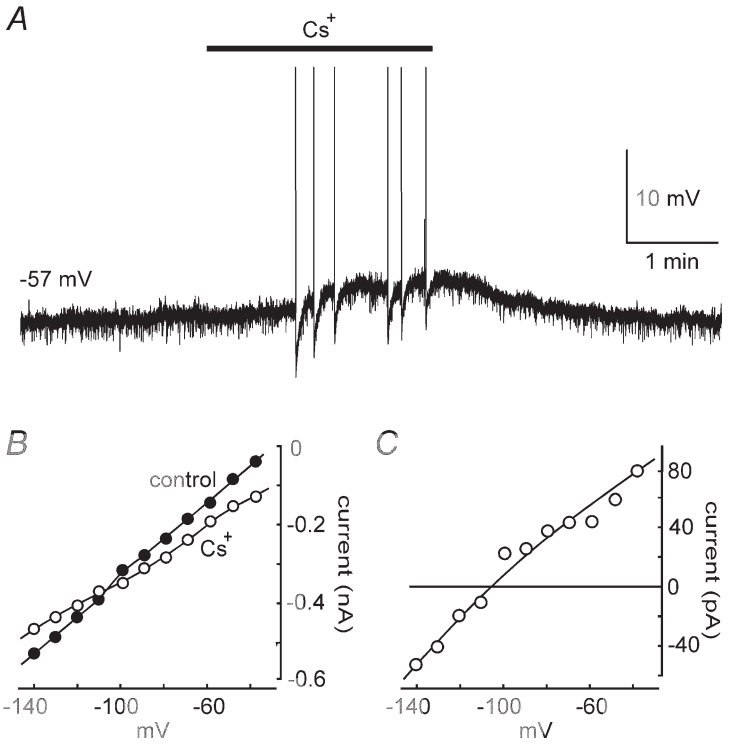

Figure 7. The Cs^+-sensitive leak current in MNCs is not blocked by TEA

A, the effect of 3 mM Cs^+ on a MNC recorded in the presence of 5 mM TEA. *B*, current–voltage plots recorded from another cell in the absence (control) and presence of 3 mM Cs^+. ZD 7288 (70 μM), TTX (0.5 μM) and TEA (5 mM) were present throughout. The graph in *C* shows the voltage dependency of the Cs^+-sensitive current obtained by subtraction of the Cs^+ from the control plot in *B*.

from blockade of I_H (e.g. Maccaferri & McBain, 1996). Moreover, in MNCs held at voltages near threshold, depolarising sags associated with voltage responses to hyperpolarising current pulses of increasing magnitude become progressively smaller as they approach −100 mV (e.g. Stern & Armstrong, 1997). This behaviour is opposite to that normally observed in cells expressing I_H (e.g. McCormick & Pape, 1990). Despite these observations, however, the existence of a functionally significant I_H in rat MNCs was recently established through the combined use of voltage-clamp analysis and bath application of ZD 7288, a selective blocker of I_H (Ghamari-Langroudi & Bourque, 2000). The analysis further suggested that the progressive reduction in sag amplitude observed during hyperpolarising responses in control conditions might be due to the deactivation of a steady-state voltage-dependent K^+ current; perhaps that which underlies slow outward rectification in rat MNCs (Stern & Armstrong, 1997). Although these studies have begun to clarify our understanding of the membrane currents expressed at near- and subthreshold voltages in rat MNCs, the ionic basis for the Cs^+-induced depolarisation remained unexplained.

Cs^+ blocks superimposed inward and outward currents in MNCs

Our voltage–current analysis indicated that the depolarising effects of bath-applied Cs^+ were associated with an increase in slope resistance, implying that ion channels are blocked, or otherwise closed, in the presence of the cation. Since membrane depolarisation results necessarily from the generation of a relative inward current, the active current being blocked by Cs^+ must be flowing in the outward direction under steady-state conditions. Analysis of the effects of Cs^+ at different steady-state voltages initially suggested the involvement of an inwardly rectifying current reversing near −85 mV. The curve plotted in Fig. 2*C*, however, reflected not only the properties of the Cs^+-sensitive conductance responsible for depolarisation, but also the effects of blocking the superimposed I_H. Indeed, our experiments showed that Cs^+ effectively blocks I_H in rat MNCs (Fig. 3) and that suppression of I_H alone imparts a strong inward rectification to the apparent voltage-dependent properties of the total Cs^+-sensitive conductance derived from *V–I* analysis (Figs 2*C* and 4).

The depolarising effects of Cs^+ are due to blockade of a leakage K^+ current

Having established that I_H blockade could confound the analysis of the conductance responsible for the production of depolarising responses, we proceeded to examine the effects of Cs^+ in the absence of I_H, by recording from MNCs in the continuous presence of 30–70 μM ZD 7288. Our results indicated that the depolarising effects of Cs^+ recorded in the absence of I_H were due to the suppression of a K^+-selective current showing only weak inward rectification, and which reversed polarity near −100 mV (Figs 6*D* and 7*C*). These observations confirm that much of the inward rectification, and the relatively positive reversal potential (−85 mV), characterising the effects of Cs^+ in control solutions is due to the simultaneous blockade of I_H (which reverses near −35 mV; Pape, 1996) and of a relatively linear leakage K^+ current (I_{KL}). Although previous studies have shown that externally applied Cs^+ can cause membrane depolarisation through the suppression of inwardly rectifying K^+ currents (Williams *et al.* 1988; Jarolimek *et al.* 1994), the present results suggest that the Cs^+-sensitive K^+ conductance in MNCs is relatively insensitive to membrane potential over the range of voltages examined (−40 to −120 mV).

Relative contributions of I_{KL} and I_H at subthreshold voltages

Our results thus show that two distinct Cs^+-sensitive conductances are present in MNCs of the rat supraoptic nucleus. Since the conductance underlying I_{KL} (G_{KL}) does not show significant voltage dependency, and since G_H becomes fully active at voltages below about −100 mV (Fig. 3*D*), the relative maximal contributions of these conductances can be approximated by an inspection of voltage–current relationships below −100 mV. In control solutions, application of Cs^+ increased membrane resistance below −100 mV from 177 to 304 MΩ. This represents the suppression of 2.36 nS of the membrane conductance active at this range of voltages. Over the same range of potentials, application of ZD 7288 was found to increase resistance from 172 to 221 MΩ. This suggests that G_H alone accounts for 1.32 nS of the steady-state membrane conductance below −100 mV. This value is similar to the maximal value of G_H derived from voltage-clamp experiments using ZD 7288 (1.1 nS; Ghamari-Langroudi & Bourque, 2000) and from an analysis of the time-dependent current blocked by Cs^+ under voltage clamp (1.2 nS; Fig. 3). The Cs^+-sensitive conductance responsible for membrane depolarisation therefore represents about 1 nS of the total membrane conductance. This estimate is supported by the finding that in the presence of ZD 7288, Cs^+ increased membrane resistance from 204 to 281 MΩ, a change corresponding to the blockade of 1.34 nS. One can surmise, therefore, that G_{KL} represents about 20 % of the input conductance of rat MNCs impaled in hypothalamic explants.

Physiological role of the Cs^+-sensitive G_{KL}

Although the MNCs from which we recorded in this study were not specifically identified as either vasopressin or oxytocin containing, it is worth emphasising that all 93 of the cells tested in our experiments displayed a Cs^+-induced response consistent with the expression of G_{KL} at rest. Since quantitative immunocytochemical studies have shown that approximately 69 % of the MNCs present in the supraoptic nucleus of Long-Evans rats (Rhodes *et al.* 1981) synthesise vasopressin while the remainder express oxytocin, it is likely that both types of neurone were sampled in our study. We can surmise,

therefore, that both types of MNC express G_{KL} at rest and that modulation of this conductance could ultimately regulate the secretion of both hormones from the neurohypophysis.

The most obvious physiological role for G_{KL} is a contribution to the resting potential. The analysis presented in the previous paragraph suggests that approximately 20 % of the input conductance of MNCs at rest is provided by steady-state Cs^+-sensitive G_{KL}. The inhibition of this resting G_{KL} by 2–5 mM Cs^+ provoked a mean membrane depolarisation of about 6 mV. Given that MNCs typically rest at voltages within 10 mV of the threshold for action potential discharge (e.g. Mason, 1983; Stern & Armstrong, 1996), the outward current normally flowing through G_{KL} channels evidently provides an important source of tonic intrinsic inhibition. Interestingly, a previous study has shown that the depolarising effects of noradrenaline are in part due to the suppression of a K^+ current that is active at the resting potential (Randle *et al.* 1985). Although it is not yet known whether these effects can be occluded by external Cs^+, the observation suggests that modulation of the inhibitory effect of G_{KL} by neurotransmitters might represent an effective mechanism for the regulation of firing and hormone release. It should also be noted that Li & Hatton (1996) previously showed that activation of histamine receptors can depolarise MNCs through the G-protein-mediated suppression of a resting voltage-independent leakage conductance. Whether histamine modulates a residual Cs^+-sensitive G_{KL} or a distinct K^+ conductance remains to be determined.

Involvement of G_{KL} in depolarising after-potentials

Another possible function for G_{KL} might be a contribution to the generation of depolarising after-potentials (DAPs). Previous studies in MNCs have shown that action potentials are followed by DAPs (Andrew & Dudek, 1983; Bourque, 1986) and that the summation of consecutive DAPs contributes to the establishment of the plateau potential that sustains firing during phasic bursts (Bourque *et al.* 1998; Ghamari-Langroudi & Bourque, 1998). Modulation of the DAP, therefore, represents a powerful mechanism for the control of firing pattern by neurotransmitters in MNCs (e.g. Papas & Bourque, 1997; Brown *et al.* 1999). A previous study has provided evidence that the DAP may result from the transient suppression of a baseline K^+ current following each action potential (Li & Hatton, 1997*b*). Although Ca^{2+} influx appears to be involved in the induction of DAPs (Bourque, 1986; Li & Hatton, 1997*a*), the nature of the putative K^+ conductance being modulated is unknown. In a previous study (Ghamari-Langroudi & Bourque, 1998) we reported that external Cs^+ effectively blocks DAPs at low millimolar concentrations. Interestingly, the blockade of DAPs during exposure to Cs^+ is accompanied by membrane depolarisation and the time course of these two effects is similar during both onset and recovery (e.g. Fig. 1 in Ghamari-Langroudi & Bourque, 1998). Since the results of the present study indicate that the Cs^+-evoked depolarisation is due to the blockade of G_{KL}, DAPs may in fact be due to a transient, action potential-evoked suppression of G_{KL} and the loss of DAPs in the presence of Cs^+ may be due to the occlusion of the basal K^+ current required for its expression. Additional studies will be required to test this hypothesis.

Molecular nature of the channels underlying G_{KL}

The participation of specialised 'leakage' K^+ channels in the regulation of resting potential has long been inferred from the observation that many transmitters regulate membrane potential through the modulation of voltage-insensitive, as opposed to voltage-activated or inwardly rectifying, K^+ conductances (Brown, 2000; North, 2000). The molecular nature of putative leakage K^+ channels has recently emerged from the cloning of several members of the two-pore K^+ channel family, such as TASK-1 (Duprat *et al.* 1997), TWIK-1 (Lesage *et al.* 1996), TREK-1 (Fink *et al.* 1996) and TRAAK (Fink *et al.* 1998). Could any of these channels underlie the G_{KL} of MNCs? Although many additional experiments will be required to provide an answer to this question, it is interesting to note that channels encoded by TASK are insensitive to TEA, but are blocked by external Cs^+ (Czirjak *et al.* 2000), as was the G_{KL} recorded in supraoptic MNCs. Moreover, TASK-1 mRNA is present in a variety of central neurones (Talley *et al.* 2000), including those in the supraoptic nucleus (E. M. Talley & D. A. Bayliss, personal communication). Whether TASK-1 or analogous channels mediate the depolarising effects of Cs^+ in MNCs remains to be determined.

Andrew, R. D. & Dudek, F. E. (1983). Burst discharge in mammalian neuroendocrine cells involves an intrinsic regenerative mechanism. *Science* **221**, 1050–1052.

Andrew, R. D. & Dudek, F. E. (1985). Spike broadening in magnocellular neuroendocrine cells of rat hypothalamic slices. *Brain Research* **334**, 176–179.

Bicknell, R. J. (1988). Optimizing release from peptide hormone secretory nerve terminals. *Journal of Experimental Biology* **139**, 51–65.

Bicknell, R. J. & Leng, G. (1981). Relative efficiency of neural firing patterns for vasopressin release *in vitro*. *Neuroendocrinology* **33**, 295–299.

Bourque, C. W. (1986). Calcium-dependent spike after-current induces burst firing in magnocellular neurosecretory cells. *Neuroscience Letters* **70**, 204–209.

Bourque, C. W. (1987). Intrinsic features and control of phasic burst onset in magnocellular neurosecretory cells. In *Organization of the Autonomic Nervous System: Central and Peripheral Mechanisms*, ed. Ciriello, J., Calaresu, F. R., Renaud, L. P. & Polosa, C., pp. 387–396. Alan R. Liss, Inc., New York.

Bourque, C. W. (1988). Transient calcium-dependent potassium current in magnocellular neurosecretory cells of the rat supraoptic nucleus. *Journal of Physiology* **97**, 331–347.

Bourque, C. W., Kirkpatrick, K. & Jarvis, C. R. (1998). Extrinsic modulation of spike afterpotentials in rat hypothalamoneurohypophysial neurons. *Cellular and Molecular Neurobiology* **18**, 3–12.

Bourque, C. W. & Renaud, L. P. (1985). Activity dependence of action potential duration in rat supraoptic neurosecretory neurons recorded *in vitro*. *Journal of Physiology* **363**, 429–439.

Bourque, C. W. & Renaud, L. P. (1991). Membrane properties of rat magnocellular neuroendocrine cells *in vivo*. *Brain Research* **540**, 349–352.

Brown, C. J., Ghamari-Langroudi, M., Leng, G. & Bourque, C. W. (1999). κ-Opioid receptor activation inhibits post-spike depolarizing after-potentials in rat supraoptic nucleus neurones *in vitro*. *Journal of Neuroendocrinology* **11**, 825–828.

Brown, D. A. (2000). Neurobiology: the acid test for resting potassium channels. *Current Biology* **10**, R456–459.

Brownstein, M. J., Russell, J. T. & Gainer, H. (1980). Synthesis, transport, and release of posterior pituitary hormones. *Science* **207**, 373–378.

Czirjak, G., Fischer, T., Spat, A., Lesage, F. & Enyedi, P. (2000). TASK (TWIK-related acid-sensitive K^+ channel) is expressed in glomerulosa cells of rat adrenal cortex and inhibited by angiotensin II. *Molecular Endocrinology* **14**, 863–874.

Dreifuss, J. J., Kalnins, I., Kelly, J. S. & Ruf, K. B. (1971). Action potentials and release of neurohypophysial hormones *in vitro*. *Journal of Physiology* **215**, 805–817.

Duprat, F., Lesage, F., Fink, M., Yeyes, R., Neurteaux, C. & Lazdunski, M. (1997). TASK, a human background K^+ channel to sense external pH variations near physiological pH. *EMBO Journal* **16**, 5464–5471.

Dutton, D. A. & Dyball, R. E. J. (1979). Phasic firing enhances vasopressin release from the rat neurohypophysis. *Journal of Physiology* **290**, 433–440.

Dyball, R. E. J., Tasker, J.-G., Wuarin, J.-P. & Dudek, F. E. (1991). *In vivo* intracellular recording of neurons in the supraoptic nucleus of the rat hypothalamus. *Journal of Neuroendocrinology* **3**, 383–386.

Erickson, K. R., Ronnekliev, O. K. & Kelly, M. J. (1993). Electrophysiology of guinea-pig supraoptic neurones: role of a hyperpolarization-activated cation current in phasic firing. *Journal of Physiology* **460**, 407–425.

Fink, M., Duprat, F., Lesage, F., Romay, G., Heurteaux, C. & Lazdunski, M. (1996). Cloning, functional expression and brain localization of a novel unconventional outward rectifier K^+ channel. *EMBO Journal* **15**, 6854–6862.

Fink, M., Lesage, F., Duprat, F., Heurteaux, C., Reyes, R., Fosset, M. & Lazdunski, M. (1998). A neuronal two P domain K^+ channel stimulated by arachidonic acid and polyunsaturated fatty acids. *EMBO Journal* **17**, 3297–3308.

Ghamari-Langroudi, M. & Bourque, C. W. (1998). Caesium blocks depolarizing after-potentials and phasic firing in rat supraoptic neurones. *Journal of Physiology* **510**, 165–175.

Ghamari-Langroudi, M. & Bourque, C. W. (2000). Excitatory role of the hyperpolarization-activated inward current in phasic and tonic firing of rat supraoptic neurons. *Journal of Neuroscience* **20**, 4855–4863.

Halliwell, J. V. & Adams, P. R. (1982). Voltage-clamp analysis of muscarinic excitation in hippocampal neurons. *Brain Research* **250**, 71–92.

Harris, N. C. & Constanti, A. (1995). Mechanism of block by ZD 7288 of the hyperpolarization-activated inward rectifying current in guinea-pig substantia nigra neurons *in vitro*. *Journal of Neurophysiology* **74**, 2366–2378.

Hatton, G. I. & Li, Z. (1998). Mechanisms of neuroendocrine cell excitability. In *Vasopressin and Oxytocin, Molecular, Cellular and Clinical Advances*, ed. Zingg, H. H., Bourque, C. W. & Bichet, D. G., pp. 79–95. Plenum Press, New York.

Jarolimek, W., Bijak, M. & Misgeld, U. (1994). Differences in the Cs block of baclofen and 4-aminopyridine induced potassium currents of guinea-pig CA3 neurons *in vitro*. *Synapse* **18**, 169–177.

Kirkpatrick, K. & Bourque, C. W. (1996). Activity dependence and functional role of the apamin-sensitive K^+ current in rat supraoptic neurones *in vitro*. *Journal of Physiology* **494**, 389–398.

Lesage, F., Guillemare, E., Fink, M., Duprat, F., Lazdunski, M., Romay, G. & Barhanin, J. (1996). TWIK-1, a ubiquitous human weakly inward rectifying K^+ channel with a novel structure. *EMBO Journal* **15**, 1004–1011.

Li, Z. & Hatton, G. I. (1996). Histamine-induced prolonged depolarization in rat supraoptic neurons: G-protein-mediated, Ca^{2+}-independent suppression of K^+ leakage conductance. *Neuroscience* **70**, 145–158.

Li, Z. & Hatton, G. I. (1997*a*). Ca^{2+} release from internal stores: role in generating depolarizing after-potentials in rat supraoptic neurones. *Journal of Physiology* **498**, 339–350.

Li, Z. & Hatton, G. I. (1997*b*). Reduced outward K^+ conductances generate depolarizing after-potentials in rat supraoptic nucleus neurones. *Journal of Physiology* **505**, 95–106.

Maccaferri, G. & McBain, C. J. (1996). The hyperpolarization-activated current (I_H) and its contribution to pacemaker activity in rat CA1 hippocampal stratum oriens–alveus interneurones. *Journal of Physiology* **497**, 119–130.

McCormick, D. A. & Pape, H. C. (1990). Properties of a hyperpolarization-activated cation current and its role in rhythmic oscillation in thalamic relay cells. *Journal of Physiology* **431**, 319–342.

Mason, W. T. (1983). Electrical properties of neurons recorded from the rat supraoptic nucleus *in vitro*. *Proceedings of the Royal Society* B **217**, 141–161.

Mayer, M. L. & Westbrook, G. L. (1983). A voltage-clamp analysis of inward (anomalous) rectification in mouse spinal sensory ganglion neurones. *Journal of Physiology* **340**, 19–45.

North, R. A. (2000). Potassium-channel closure taken to TASK. *Trends in Neurosciences* **23**, 234–235.

Papas, S. & Bourque, C. W. (1997). Galanin inhibits continuous and phasic firing in rat hypothalamic magnocellular neurosecretory cells. *Journal of Neuroscience* **17**, 6048–6056.

Pape, H. C. (1996). Queer current and pacemaker: the hyperpolarization-activated cation current in neurons. *Annual Review of Physiology* **58**, 299–327.

Poulain, D. A. & Wakerley, J. B. (1982). Electrophysiology of hypothalamic magnocellular neurones secreting oxytocin and vasopressin. *Neuroscience* **7**, 773–808.

Randle, J. C. R., Bourque, C. W. & Renaud, L. P. (1985). α1-Adrenergic receptor activation depolarizes rat supraoptic neurosecretory neurons *in vitro*. *American Journal of Physiology* **251**, R569–574.

Renaud, L. P. & Bourque, C. W. (1991). Neurophysiology and neuropharmacology of hypothalamic magnocellular neurons secreting vasopressin and oxytocin. *Progress in Neurobiology* **36**, 131–169.

Rhodes, C. H., Morrell, J. I. & Pfaff, D. W. (1981). Immunohistochemical analysis of magnocellular elements in rat hypothalamus: distribution and numbers of cells containing neurophysin, oxytocin and vasopressin. *Journal of Comparative Neurology* **198**, 45–64.

Stern, J. E. & Armstrong, W. E. (1996). Changes in the electrical properties of supraoptic oxytocin and vasopressin neurons during lactation. *Journal of Neuroscience* **16**, 4861–4871.

Stern, J. E. & Armstrong, W. E. (1997). Sustained outward rectification of oxytocinergic neurones in the rat supraoptic nucleus: ionic dependence and pharmacology. *Journal of Physiology* **500**, 497–508.

Talley, E. M., Lei, Q., Sirois, J. E. & Bayliss, D. A. (2000). TASK-1, a two pore domain K^+ channel, is modulated by multiple neurotransmitters in motoneurons. *Neuron* **25**, 399–410.

Tasker, J. G. & Dudek, F. E. (1991). Electrophysiological properties of neurones in the region of the paraventricular nucleus in slices of rat hypothalamus. *Journal of Physiology* **434**, 271–293.

Williams, J. T., Colmers, W. F. & Pan, Z. Z. (1988). Voltage- and ligand-activated inwardly rectifying currents in dorsal raphe neurones *in vitro*. *Journal of Neuroscience* **8**, 3499–3506.

Acknowledgements

This work was supported by an operating grant from the Canadian Institutes of Health Research and by an MRC Senior Scientist Award to C.W.B.

Corresponding author

C. W. Bourque: L7-216, Montreal General Hospital, 1650 Cedar Avenue, Montreal, QC, Canada H3G 1A4.

Email: charles.bourque@mcgill.ca